

Topotactic relations among pyrolusite, manganite, and Mn_5O_8 : A high-resolution transmission electron microscopy investigation

JAMES H. RASK

Department of Geology, Arizona State University, Tempe, Arizona 85287

PETER R. BUSECK

Departments of Geology and Chemistry, Arizona State University,
Tempe, Arizona 85287

ABSTRACT

Pyrolusite (MnO_2 , tetragonal) is commonly created in the natural environment by the oxidation of manganite ($MnOOH$, monoclinic). Such secondary pyrolusite typically displays anomalous, nontetragonal characteristics. In this high-resolution transmission electron microscopy (HRTEM) study, Mn_5O_8 (monoclinic) was found intergrown with pyrolusite that had formed from manganite. This occurrence of Mn_5O_8 is of interest for several reasons: (1) Mn_5O_8 has been identified in a natural manganite-pyrolusite mixture. Assuming that it is not an artifact of HRTEM observation, this is the first report of naturally occurring Mn_5O_8 . (2) Aligned monoclinic Mn_5O_8 intergrown with pyrolusite may be partly responsible for the nontetragonal character of secondary pyrolusite. (3) Mn_5O_8 -pyrolusite intergrowths occur adjacent to manganite. This occurrence suggests that the oxidation of manganite may form both pyrolusite and Mn_5O_8 .

Another new Mn oxide has been identified through selected-area electron diffraction. We hypothesize that this phase is a structural modification of pyrolusite. Ordering of OH groups and Mn atoms of different oxidation states is a possible explanation for this modification.

INTRODUCTION

Pyrolusite (MnO_2), a tetragonal mineral with the rutile structure, is the most stable form of manganese oxide in many terrestrial environments. Distinctions have long been recognized between the relatively rare primary form of pyrolusite and the much more common secondary form that occurs as pseudomorphic replacements of other manganese oxide minerals, particularly manganite ($MnOOH$, monoclinic). Primary pyrolusite has a hardness of 7, whereas secondary pyrolusite displays variable, much lower hardness values. Secondary pyrolusite also possesses several characteristics suggestive of a symmetry lower than tetragonal. For example, reflected-light microscopy shows only one cleavage direction as well as optical anisotropy in the (001) plane of secondary pyrolusite. Until Strunz (1943) showed through single-crystal X-ray measurements that the two forms of pyrolusite have identical crystal structures, primary pyrolusite was termed polianite and considered a distinct mineral. Later studies (de Wolff, 1959; Potter and Rossman, 1979) have found that some secondary pyrolusites are actually orthorhombic.

Another anomalous property of secondary pyrolusite, termed the memory effect, was noted by Dent Glasser and Smith (1968). Ideally, pyrolusite has two equivalent lattice

translations, a_1 and a_2 . Either of these should have an equal probability of becoming the manganite a (or b) translation when pyrolusite is reduced to manganite. However, that is not what is observed. In the sequence manganite (primary) \rightarrow pyrolusite (secondary) \rightarrow manganite (secondary), primary and secondary manganite invariably have the same orientations. A memory of the original manganite orientation is conveyed by the pyrolusite intermediate, but there is a question as to how this memory is transmitted.

The nontetragonal characteristics of secondary pyrolusite have been attributed to microstructures formed in pyrolusite upon its creation from manganite (Strunz, 1943; Champness, 1971). Pyrolusite and manganite have similar structures. The manganite a and c translations are halved to form the a and c pyrolusite unit-cell translations, while b of manganite contracts from 5.28 Å to 4.40 Å to form the other a translation of pyrolusite (Fig. 1). This 15% contraction along b presents the possibility that microscopic cracks paralleling the manganite (010) planes separate newly made crystallites of pyrolusite. Images obtained by transmission electron microscopy confirm the existence of lamellar micropores in secondary pyrolusite (Champness, 1971). Such microcracks may explain the aberrant optical properties, the decreased hardness, and the great chemical activity and adsorptivity of secondary

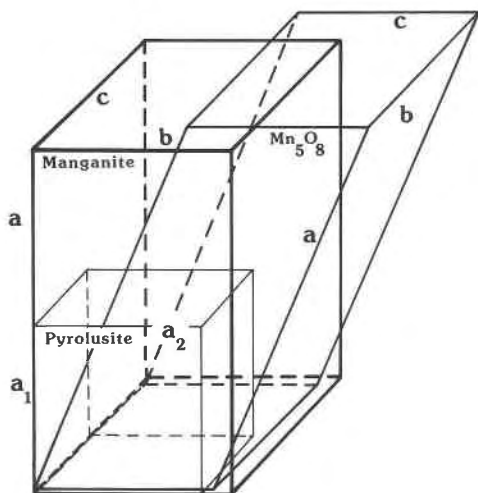


Fig. 1. A drawing to illustrate the dimensions of the pyrolusite, manganite, and Mn_5O_8 unit cells and their relative orientations in the topotactic reactions.

pyrolusite, but probably cannot explain observed slight deviations of such pyrolusite from tetragonal symmetry. The memory effect may also be a result of these aligned lamellar microcracks.

Here we report the findings of high-resolution transmission electron microscopy (HRTEM) examinations of unheated natural mixtures of manganite and pyrolusite and similar examinations of portions of these mixtures heated in air to 300°C. We have observed micropores, as reported by Champness (1971), but we have also determined that an intermediate phase, Mn_5O_8 ($Mn_3^{2+}Mn_2^{4+}O_8$), plays an important role in the anomalous behavior of some secondary pyrolusite. Our discovery of Mn_5O_8 in unheated, ion-milled, natural samples is of additional interest because Mn_5O_8 in a natural occurrence has not previously been reported. Furthermore, since Mn_5O_8 is an intermediate phase in oxidation and reduction reactions of Mn oxides, it should be given consideration in studies of Mn-oxide phase equilibria.

EXPERIMENTAL DETAILS

The specimens studied are from the Stanford University mineral collection. They are labeled as manganite originating from the Lake Superior region (sample no. 51110) and from Ilfeld, Harz, Germany (sample no. 7152). Powder X-ray diffraction (XRD) revealed these specimens to be mixtures of pyrolusite and manganite. To continue the reaction of manganite to pyrolusite, portions of the specimens were powdered and heated in air for 1.5 to 3 h. An XRD powder pattern of a sample that had been heated at 300°C for 3 h showed no manganite reflections. This pattern contained, along with strong pyrolusite peaks, less intense reflections attributable to Mn_5O_8 . Both heated and unheated samples were examined by HRTEM as grains mounted on holey-carbon film. To obtain better observations of the relationships among intergrown phases, an ion-thinned sample of the Lake Superior specimen was prepared and observed before and after heating. In the milling process, ionized argon bombards the sample in an evacuated chamber. The Lake Superior manganite was ion-milled

Table 1. Unit-cell dimensions of pyrolusite, manganite, and Mn_5O_8

Pyrolusite	Manganite	Mn_5O_8
$a = 4.3999 \text{ \AA}$	$a = 8.98 \text{ \AA}$	$a = 10.347 \text{ \AA}$
$c = 2.8740 \text{ \AA}$	$b = 5.28 \text{ \AA}$	$b = 5.72 \text{ \AA}$
	$c = 5.71 \text{ \AA}$	$c = 4.852 \text{ \AA}$
	$\beta = 90^\circ$	$\beta = 109^\circ 25'$
SG = $P4_2/mnm$ (#136)	SG = $B2_1/d$ (#14)	SG = $C2/m$ (#12)
Source :	Source :	Source :
Bauer, 1976	Buerger, 1936	Oswald and Wampetich, 1967

for 20 h at 5 kV and for 2 h at 1.5 kV. A JEOL-JEM 200CX 200-kV and a Philips 400T 120-kV microscope were the instruments used in this study.

CRYSTALLOGRAPHIC RELATIONS AMONG MANGANITE, PYROLUSITE, AND Mn_5O_8

The unit cells of pyrolusite, manganite, and Mn_5O_8 are closely related (Baur, 1976; Buerger, 1936; Oswald et al., 1967), and in their topotactic transformations, their crystallographic axes remain in nearly the same relative orientations. The a , b , and c axes of manganite correspond directly to the a axes and the c axis of pyrolusite. The a axis of Mn_5O_8 is at an angle of 19° from one a axis of pyrolusite and a of manganite; b of Mn_5O_8 corresponds to the c translation of pyrolusite and manganite; and c of Mn_5O_8 has the same orientation as b of manganite, and a of pyrolusite (Dent Glasser and Smith, 1968). Pertinent crystallographic data are given in Table 1, and the orientation relations among the unit cells of these minerals are illustrated in Figure 1.

Since manganite has perfect (010) cleavage, crushed grain mounts commonly contain manganite particles oriented with the [010] zone axis nearly parallel to the electron beam. The ion-thinned sample also was examined only in this orientation. The preponderance of this orientation has advantages and disadvantages. Although the changes from manganite to pyrolusite and Mn_5O_8 are clearly evident in the selected-area electron diffraction (SAED) patterns taken from this orientation, micropores that parallel the manganite (010) planes are not observable.

SAED patterns of these minerals, all in the orientation corresponding to [010] of parent manganite, are illustrated in Figure 2. The reflections along the a^* direction are virtually identical in the manganite [010] and the pyrolusite [010] diffraction patterns. However, the manganite (101) spacing is double that of pyrolusite, so the $\bar{1}01$ and $10\bar{1}$ manganite reflections appear halfway between the origin and the more intense spots that correspond to the pyrolusite $\bar{1}01$ and $10\bar{1}$ reflections (in the manganite patterns these are the $\bar{2}02$ and $20\bar{2}$ reflections). The 101 , $\bar{1}0\bar{1}$, 200 , and $\bar{2}00$ reflections do not appear in the manganite pattern because of the $h + l = 4n$ requirement for allowed $h0l$ reflections imposed by the diamond glide in the manganite structure.

The [001] Mn_5O_8 pattern was commonly observed to

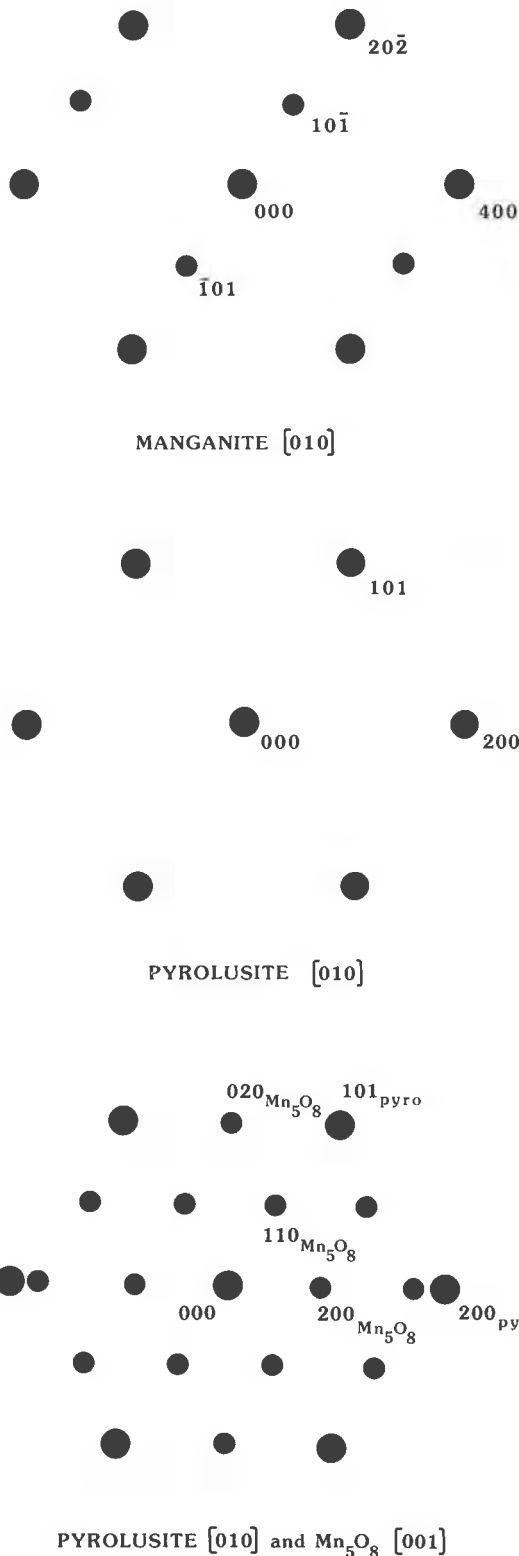


Fig. 2. Illustrations of pyrolusite, manganite, and Mn_5O_8 SAED patterns. The orientation of each of these SAED patterns corresponds to the [010] orientation of parent manganite. This is the orientation of all subsequent HRTEM images of pyrolusite, manganite, and Mn_5O_8 .

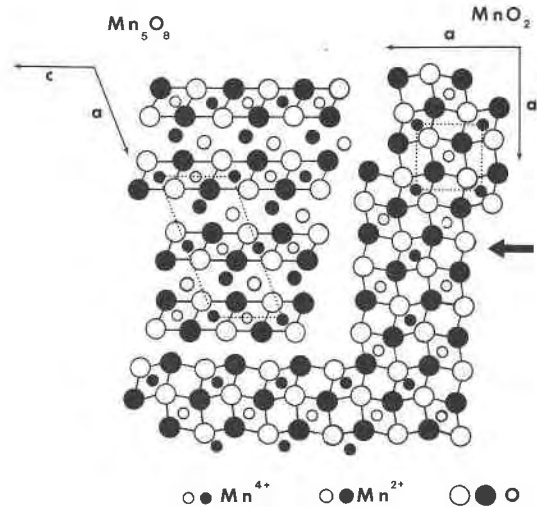


Fig. 3. A schematic illustration of a Mn_5O_8 -pyrolusite intergrowth as seen looking down the pyrolusite [001] axis (Mn_5O_8 [010]). Unit-cell boundaries are shown by dotted lines. The representations of pyrolusite and Mn_5O_8 are adapted from Dent Glasser and Smith (1967). In the illustration of pyrolusite, filled circles represent oxygen and Mn^{4+} at $1/2c$; open circles represent oxygen and Mn^{4+} at $c = 0$. In the Mn_5O_8 illustration, open circles represent oxygen at $b = 0, 0.50b$; Mn^{4+} at $b = 0$; and Mn^{2+} at $b = 0$; whereas filled circles represent oxygen at $0.25b, 0.75b$; Mn^{4+} at $0.25b, 0.75b$; and Mn^{2+} at $0.50b$. Note that b of Mn_5O_8 is approximately twice the length of c in pyrolusite. Therefore, in the third dimension of this illustration, the oxygens are at similar heights in the two structures, as are the Mn^{4+} ions. HRTEM images of Mn_5O_8 -pyrolusite intergrowths shown in subsequent figures are looking down the pyrolusite [010]- Mn_5O_8 [001] axis. The bold arrow to the right of the illustration indicates this viewing direction.

be superimposed on a more intense pyrolusite [010] pattern, indicating an intergrowth relationship between these two phases. In such patterns, the 200 reflection of Mn_5O_8 is located slightly less than halfway between the central spot and the pyrolusite 200 reflection (Mn_5O_8 $d_{200} = 4.88$ Å and pyrolusite $d_{100} = 4.40$ Å). Thus, the Mn_5O_8 200 reflection is readily distinguished from the 100 reflection of pyrolusite that, though kinematically forbidden, appears in some diffraction patterns of these intergrowths. In intergrowths of pyrolusite and well-crystallized Mn_5O_8 , diffraction spots representing Mn_5O_8 (110), $(\bar{1}\bar{1}0)$, $(\bar{1}10)$, and $(1\bar{1}0)$ planes appear approximately halfway between the origin and diffraction spots representing pyrolusite (101), $(\bar{1}0\bar{1})$, $(\bar{1}01)$, and $(10\bar{1})$ planes.

Mn_5O_8 : A NEW MINERAL?

Klingsberg and Roy (1960), in a study of the Mn-O system, recognized a new compound in several of their run products. It is apparent from their published XRD data that the compound is Mn_5O_8 . Oswald et al. (1965) used $\text{Cd}_2\text{Mn}_5\text{O}_8$ as a model to index the XRD pattern of Mn_5O_8 . The structure of Mn_5O_8 , as determined by Oswald and Wampetich (1967), is based on layers of edge-shared

MnO₆ octahedra. Thus, in the classification scheme proposed by Turner and Buseck (1981), Mn₅O₈ is a 1×∞ Mn oxide. One quarter of the octahedral positions in these layers are vacant. Mn²⁺ atoms occupy interlayer sites adjacent to the vacant octahedra. Several methods by which Mn₅O₈ may be synthesized have been reported (Klingsberg and Roy, 1959; Oswald et al., 1965; Feitknecht, 1964; Dasgupta, 1965; Davis, 1967). Burns and Burns (1979) included Mn₅O₈ in their review of Mn oxides.

Identification of Mn₅O₈ in unheated, natural samples is significant because such an occurrence has not been previously reported. We have identified poorly crystallized Mn₅O₈ intergrown with pyrolusite in the unheated, ion-milled Lake Superior manganite sample. SAED patterns and high-resolution images from the pyrolusite [010], Mn₅O₈ [001] orientation suggest that the octahedral layers of Mn₅O₈ are intermeshed with the 1×1 octahedral tunnel structure of pyrolusite, as illustrated schematically in Figure 3. The 4.40-Å tunnel dimension of pyrolusite, corresponding to *d*₁₀₀, is significantly smaller than its counterpart in Mn₅O₈, the 4.88-Å interlayer dimension that corresponds to *d*₂₀₀. Accommodations for this misfit must be present in these intergrowths. Because no high-resolution images have been obtained from the necessary orientation ([001] pyrolusite, [010] Mn₅O₈), the nature of such accommodations is unknown.

Our identification of Mn₅O₈ from unheated samples is based totally on HRTEM, which has the inherent possibility that samples may be altered upon interaction with the electron beam. Also, alteration of manganite could have occurred during ion-milling. Thus we cannot conclude unequivocally that Mn₅O₈ occurs in nature. In fact, when an electron beam of maximum intensity (achieved by removal of the condenser aperture) is focused on a particle of manganite, the manganite is quickly transformed to Mn₅O₈.

We believe, however, that most of the Mn₅O₈ that we observed was not formed through such decomposition of manganite in the electron beam. Experience has shown that manganite is relatively stable under a beam in the usual configuration (condenser aperture in). Also, Mn₅O₈ created from manganite by an intense electron beam is pure, whereas most Mn₅O₈ observed under normal beam conditions is intergrown with pyrolusite. Finally, Mn₅O₈ unquestionably increased in abundance after the samples were heated outside the microscope. This increase, noted in XRD as well as HRTEM results, proves that the Mn₅O₈ under consideration is not solely an artifact of HRTEM observation.

We have yet to detect Mn₅O₈ in unheated samples by

XRD, and it is not evident in any of several published XRD patterns of secondary pyrolusite (Potter and Rossman, 1979; de Wolff, 1959). Even if present, Mn₅O₈ may elude XRD detection because of poor crystallinity or scarcity. However, given the easy synthesis of Mn₅O₈ from the relatively common mineral manganite, it seems likely that Mn₅O₈ does have natural occurrences.

ORIENTED INTERGROWTHS OF PYROLUSITE AND Mn₅O₈

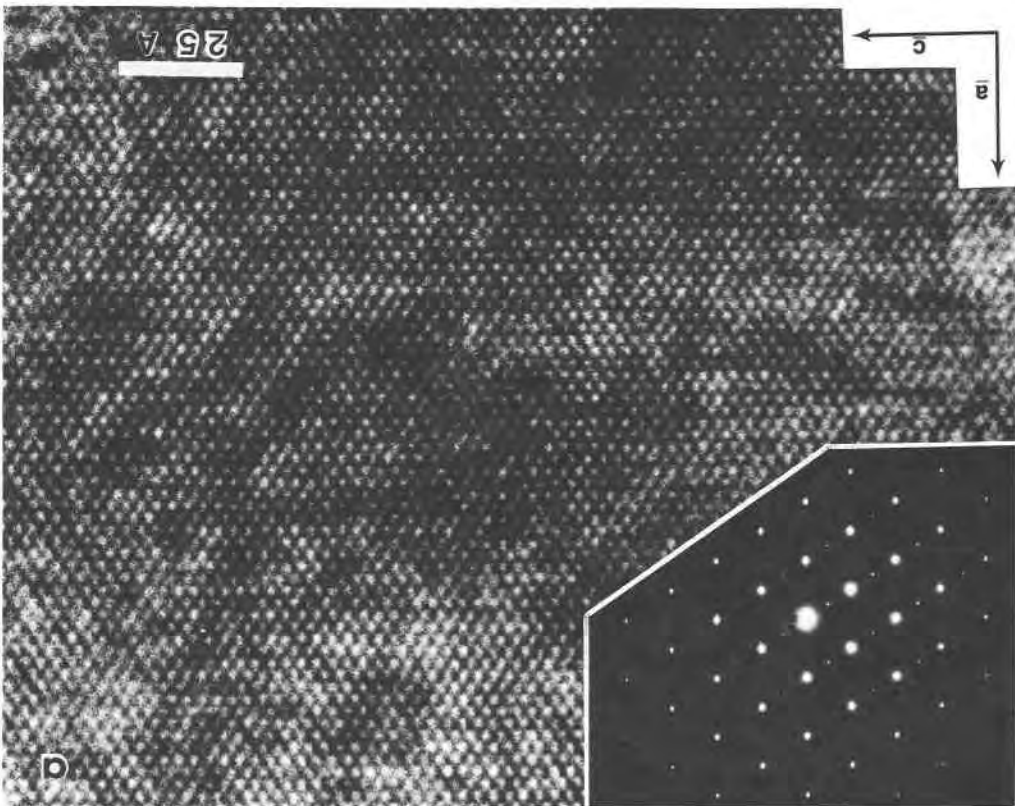
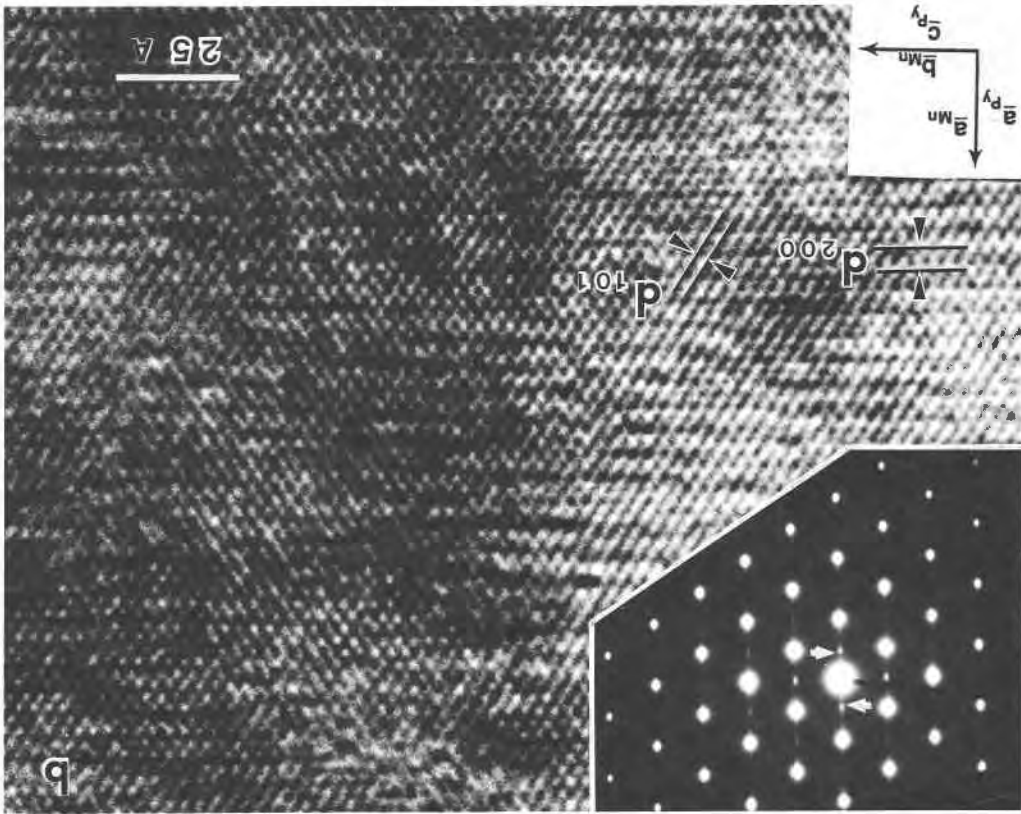
Figure 4 shows electron-diffraction patterns and images taken from the unheated ion-milled sample of the Lake Superior manganite. This sample consists of domains of manganite and domains of pyrolusite intergrown with poorly crystalline Mn₅O₈. The domains are at slightly differing (±5°) orientations, all near to the [010] pyrolusite-[010] manganite-[001] Mn₅O₈ orientation. Figure 4a shows an image and SAED pattern of manganite. In the image mode, manganite can be recognized by a uniform appearance, with little evidence of crystal strain or defects. Pyrolusite-Mn₅O₈ intergrowths typically have a mottled appearance, probably as a response to crystal strain incurred during the manganite-to-pyrolusite transition.

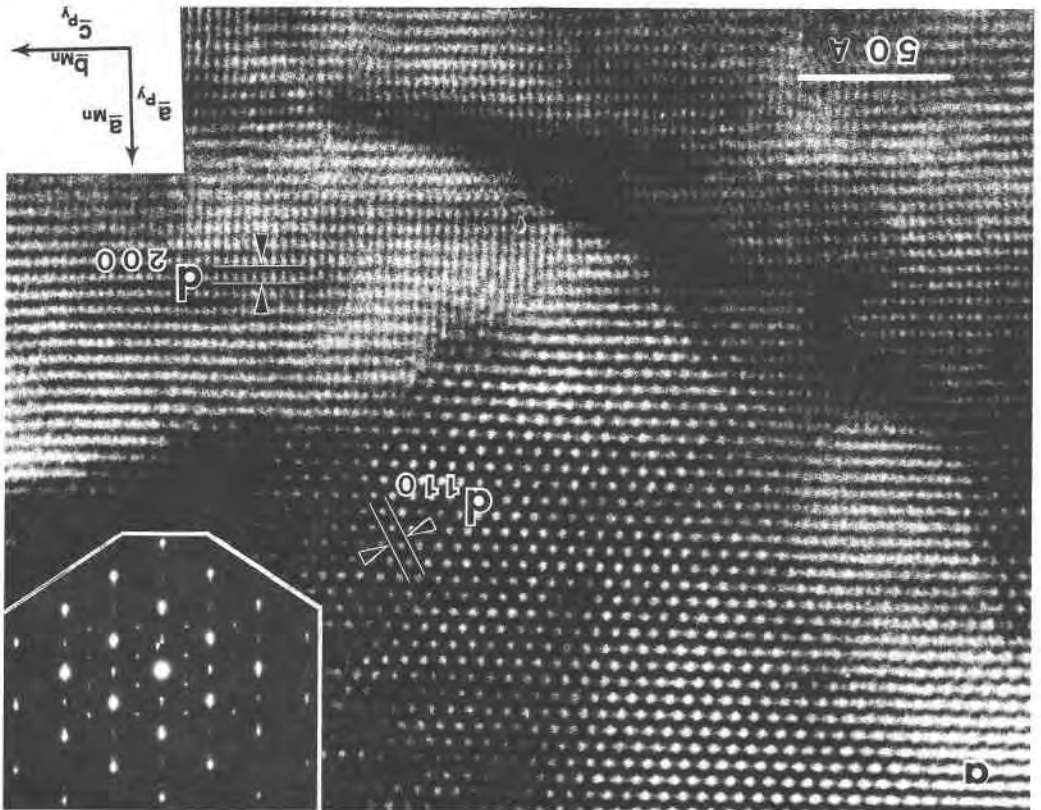
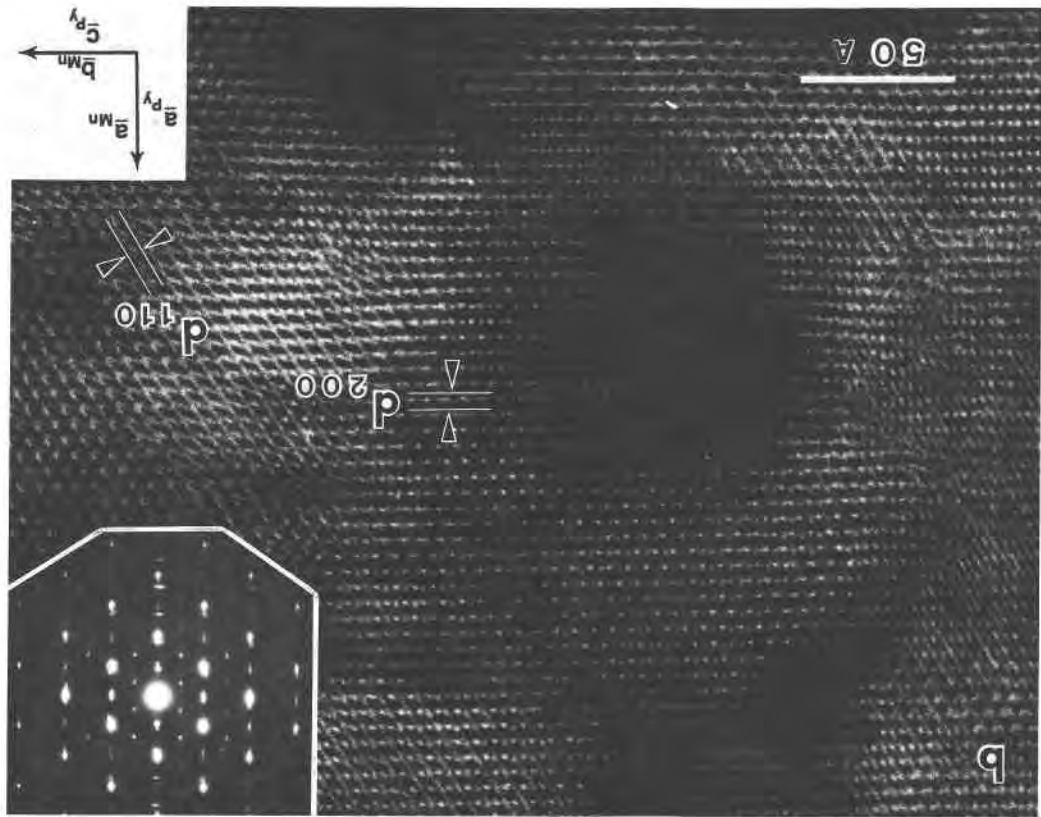
Intergrowths of pyrolusite and poorly crystalline Mn₅O₈ occur adjacent to manganite. Figure 4b shows a high-resolution image of such an intergrowth and its SAED pattern, which is a strong pyrolusite [010] pattern with additional weaker reflections along *a**. The weak 4.9-Å reflections and the corresponding lattice fringes of the image are interpreted as representing the (200) planes of Mn₅O₈ and provide the evidence for Mn₅O₈ in this unheated sample. The lack of Mn₅O₈ 110 spots (as occur in the SAED patterns in Fig. 5) suggests Mn₅O₈ is ordered well enough to produce distinct SAED reflections only along *a**. The ordering along *b*, involving vacancies in the layers and interlayer Mn²⁺, is poorly developed.

MnO₂ with the diaspore structure (ramsdellite in its pure form) forms intergrowths on the unit-cell scale with pyrolusite (de Wolff, 1959; Giovanoli et al., 1967). Naturally occurring specimens of this intergrowth are called nsutite, while synthetic preparations of it are termed γ-MnO₂. We are confident that the phase intergrown with pyrolusite in Figure 4b is Mn₅O₈ and not ramsdellite. The 4.9-Å spacing of the weak spots along *a** in our SAED patterns is too large to attribute to the only plausible ramsdellite spacing, *d*₀₂₀ = 4.64 Å. Also, the *a** direction in SAED patterns of unheated samples is identical to the *a** direction seen in SAED patterns of definite Mn₅O₈-pyrolusite intergrowths from heated samples.

Intergrowths of pyrolusite and well-crystallized Mn₅O₈

Fig. 4. SAED patterns and micrographs of the unheated, ion-thinned Lake Superior specimen of pyrolusite and manganite. (a) SAED pattern and image of manganite in the [010] orientation. The sets of fringes that run diagonally across the image correspond to manganite (202) and (20 $\bar{2}$) spacings (2.4 Å) (b) Corresponding SAED pattern and image of intergrown pyrolusite (zone [010]) and Mn₅O₈ (zone [001]). Reflections that represent Mn₅O₈ (200) planes (marked by arrows) have appeared at 4.9 Å⁻¹ along *a**. Streaking along *a** in this SAED pattern indicates that disorder is present along the *a* direction of Mn₅O₈ or pyrolusite. In the HRTEM image, horizontal fringes representing Mn₅O₈ *d*₂₀₀ are superimposed upon the diagonal pyrolusite (101) and (10 $\bar{1}$) fringes.





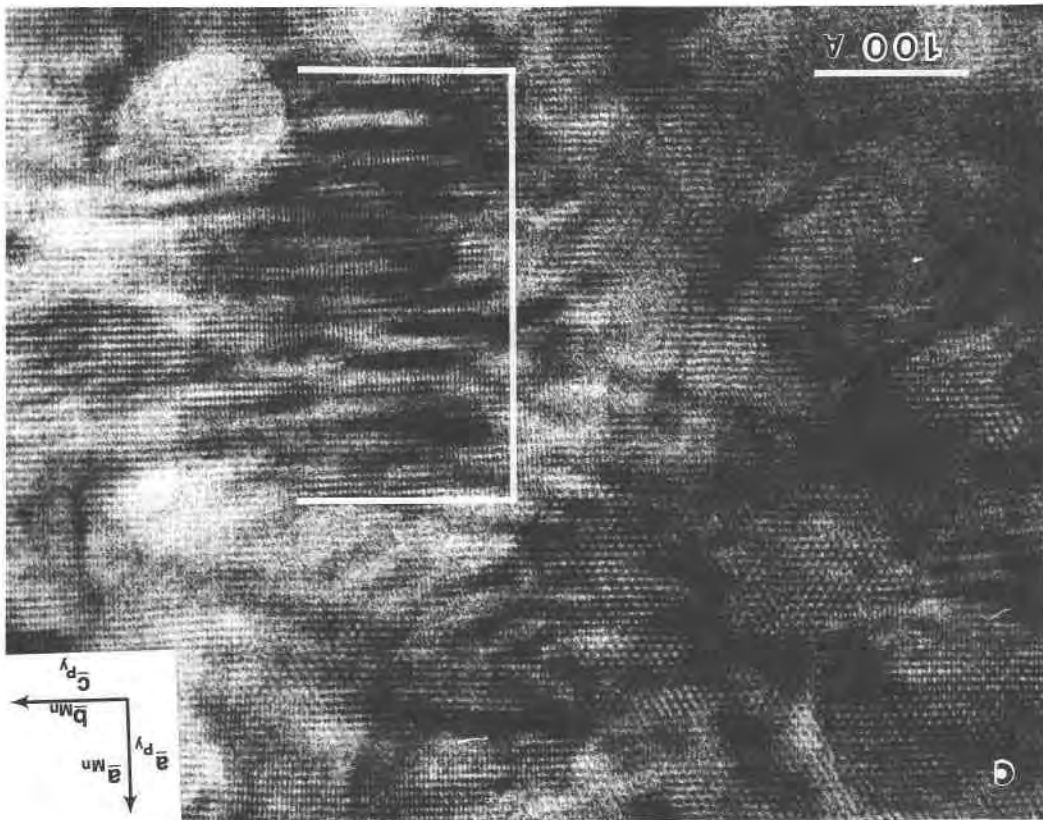


Fig. 5. SAED patterns and micrographs of pyrolytized-Mn₂O₃ intergrowths. These intergrowths were observed in the ion-thinned Lake Superior specimen of pyrolytized and manganese after heating in air. (a, left) Mn₂O₃-pyrolytized intergrowths in sample heated for 1.5 h at 200°C. The upper portion of the image that has a honeycomb-like appearance is interpreted as pure, well-crystallized Mn₂O₃. The diagonal fringes represent (110) and (110) of Mn₂O₃. The lower portion of the image probably represents an area of intermixed Mn₂O₃ and pyrolytized. The horizontal fringes represent Mn₂O₃ (200) planes. (b, left) Analogous intergrowths in the same sample heated an additional 2.5 h at 300°C. Again, the diagonal fringes represent Mn₂O₃ (110), whereas the horizontal fringes represent Mn₂O₃ (200). (c, above) Mn₂O₃-pyrolytized intergrowths in sample heated for 1.5 h at 200°C. Moiré fringes that result from the misfit between pyrolytized d_{100} and Mn₂O₃ d_{200} are indicated by a bracket.

that pyrolytized-Mn₂O₃ intergrowths occur as described above. According to Pashley et al. (1957), Moiré fringes result from "coincidence of the projected planes of atoms in two overlapping lattices." The spacing, *sp*, of such fringes is given by the equation:

$$(1) \quad sp = (d_1 + d_2)/(d_1 - d_2)$$

where d_1 and d_2 are spacings of planes in the overlapping lattices. Furthermore, relative misorientations of the overlapping lattices result in a rotation of the Moiré fringes about the viewing axis of an angle, *W*:

$$(2) \quad W = \alpha d_1 / (d_1 - d_2)$$

where α is the angle of misorientation. Equation 1 gives a spacing of 19.3 Å if we assume that the overlapping spacings responsible for the Moiré fringes in Figure 5c are 4.88 Å (d_{200} for Mn₂O₃) and 4.40 Å (d_{100} for pyrolytized—supposedly exact, but actually present in the SAED pattern of Fig. 5c). This value is within experimental error of the measured spacings of these fringes, 18

of Mn₂O₃. The Moiré fringes in Figure 5c provide added evidence of Mn₂O₃. involves heating of manganese and, presumably, creation may be especially important for the memory effect, which characteristics of secondary pyrolytized. The alignment of Mn₂O₃ tergrowths that may help cause the nontrigonal character of Mn₂O₃ in- introduces an anisotropy into the pyrolytized-Mn₂O₃ in- [001] orientation. Such alignment of monoclinic Mn₂O₃ ganite and pyrolytized in their [010] orientations) is in the heated ion-thinned sample (which was originally man- All Mn₂O₃ observed intergrown with pyrolytized in the increase as the heating is increased (Fig. 5b). relative to the pyrolytized-Mn₂O₃ intergrowths appears to luster and Mn₂O₃. The amount of well-crystallized Mn₂O₃ images occur as islands in larger areas of intergrown pyro- that produce two-dimensional, honeycomb-like HRTEM samples (Figs. 5a, 5b). Well-crystallized areas of Mn₂O₃ is better ordered and more abundant than in unheated entation in all heated samples. In such samples, Mn₂O₃ ori- were observed in the pyrolytized [010]-Mn₂O₃ [001] ori-

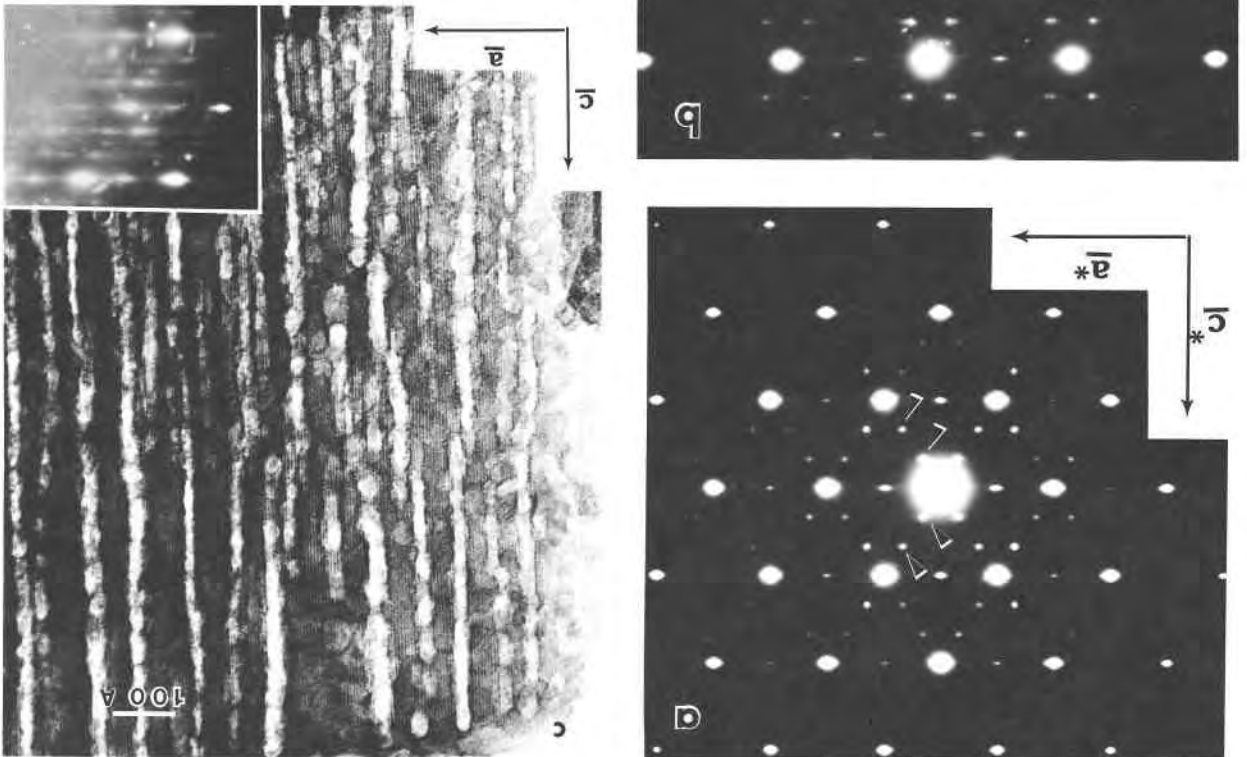
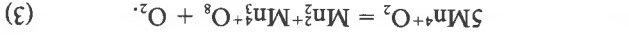


Fig. 6. SAED patterns and a micrograph of an unknown Mn oxide that, for convenience, we have termed phase M. The intense subcell seen in the SAED patterns corresponds to the [100] (or [010]) SAED pattern of pyrolusite. The axes placed on these SAED patterns refer to this pyrolusite subcell. (a) An SAED pattern from a particle in a crushed-grain mount of a standard pyrolusite sample, IC no. 6. The most intense reflections are identical to those in the pyrolusite [010] pattern. The reflections that denote phase M intersect [101]* of the pyrolusite subcell and are marked with arrows. (b) Analogous diffraction pattern from a natural sample, heated in air at 300°C for 2 h. The reflections denoting phase M are marked with arrows, as in Fig. 6a. (c) An unheated grain of the Ilfeld, Harz, manganese specimen that shows a striking micropore morphology and an SAED pattern with the weak tripling along [101]* that is indicative of phase M.

heating in air show well-crystallized Mn_3O_8 occurring in-tergrown with pyrolusite and growing from pyrolusite as heating is increased. This growth of Mn_3O_8 from pyro-lusite confirms the finding (Dent Glasser and Smith, 1968) that in air at temperatures above 300°C, Mn_3O_8 forms from secondary pyrolusite, not from manganese. The re-action of pyrolusite to Mn_3O_8 can be written



Our observation of poorly crystalline Mn_3O_8 intergrown with pyrolusite in an unheated natural mixture of pyro-lusite and manganiite suggests that Mn_3O_8 may coexist with manganiite and pyrolusite in certain diagenetic en-vironments. In the related reaction of ramsdellite to grout-ite ($MnOOH$), Klingsberg and Roy (1959) found an in-

A. Additionally, since these Moiré fringes parallel the Mn_3O_8 (200) lattice fringes, Equation 2 indicates that, as expected, there is no rotation between the Mn_3O_8 (100) planes and the pyrolusite (100) planes.

IMPLICATIONS FOR REACTIONS IN Mn-O-H₂O SYSTEM

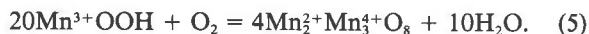
The phase transformations of manganiite upon heating in air show an interesting feature in that Mn is first oxi-dized—in the $MnOOH$ to MnO_2 transition—but, upon further heating, Mn is reduced as MnO_2 goes to Mn_2O_3 and finally to Mn_3O_4 . Mn_3O_8 is well established as an intermediate phase in this progression (Oswald et al., 1965), forming between MnO_2 and Mn_2O_3 at or above 300°C. HRTEM observations of the Lake Superior specimen after

intermediate phase (not Mn_5O_8) and tentatively named it groutellite. In their study of the manganite-to-pyrolusite reaction, they found no such intermediate phase. However, their identifications relied solely on XRD, which we also found to provide no evidence of intermediate Mn_5O_8 . Our SAED patterns of an unheated pyrolusite-manganite mixture provide evidence that Mn_5O_8 is present with pyrolusite and manganite at low temperatures.

The reaction of manganite to pyrolusite may be written as



Strunz (1943) stated that the most likely mechanism for this reaction is migration of H out of manganite, rather than O influx into manganite. However, in the absence of mechanistic evidence, we have chosen to write this oxidation reaction in the more conventional manner. Our finding of low-temperature Mn_5O_8 -pyrolusite intergrowths in close proximity to manganite suggests that Mn_5O_8 may also be formed from manganite decomposition by a reaction such as



Reactions 4 and 5 may operate simultaneously, the proportion of pyrolusite to Mn_5O_8 depending on local variations in oxygen fugacity. Crystallite size is a further factor in controlling such reactions, as was shown by Giovanoli and Leuenberger (1969) for the oxidation of α - $MnOOH$ (groutite). The micropores that develop parallel to manganite (010) as a result of these reactions may provide channels for the escape of H_2O . They may also facilitate migration of oxygen into the crystal and thus oxidation and elimination of Mn_5O_8 by the reverse of Reaction 3.

NEW Mn OXIDE

In the course of this study, we have discovered a previously unreported Mn oxide phase henceforth termed "phase M." This phase is identified by diffraction patterns that have strong reflections exactly corresponding to those in the [010] pattern of pyrolusite and weak reflections that trisect the (101) and (10 $\bar{1}$) spacings of the dominant pyrolusite pattern (Figs. 6a, 6b). The weak reflections denote a periodicity of 7.2 Å in the pyrolusite [101] direction. Pyrolusite, manganite, and Mn_5O_8 do not have spacings close to 7.2 Å, and we have found no other Mn oxide structure that appears appropriate.

Phase M has been found in crushed grain mounts of the heated Lake Superior sample; of the unheated Ilfeld, Harz, sample; and of standard pyrolusite sample IC no. 6 (Kozawa, 1981). In unheated Ilfeld manganite, the unknown phase occurs in a grain that shows a pronounced micropore morphology (Fig. 6c). Assuming that these micropores parallel (010) of a parent manganite, the 4.7-Å spacing of the lattice fringes paralleling the micropores presumably represents the lattice translation of phase M that formed from the 5.28-Å *b* translation of manganite.

Two obvious explanations for these extra reflections can be immediately discounted. They are not a result of an

ordered entry of another element (except, perhaps, H) into the pyrolusite structure. Electron energy-loss spectroscopy and energy-dispersive X-ray emission spectroscopy detected no elements other than Mn and O in this phase. Nor do they indicate large tunnel structures, common in some Mn oxides (Turner and Buseck, 1981). Such large tunnel dimensions would be made evident by additional reflections along a^* , not along [101].

We believe that the 7.2-Å spacing of phase M may be a result of ordering along the [101] direction involving OH groups and Mn atoms of different oxidation states. Analogous doubling along [101] marks the difference in Mn oxidation between manganite and pyrolusite; tripling along [101] in phase M may also signal a different average Mn oxidation state.

CONCLUSIONS

HRTEM study of natural mixtures of pyrolusite and manganite before and after heating has resulted in the following findings: (1) Mn_5O_8 has been identified through electron diffraction and imaging in unheated natural pyrolusite-manganite mixtures. In such specimens, Mn_5O_8 occurs as a poorly crystalline phase intergrown with pyrolusite. This represents the first reported identification of Mn_5O_8 in natural samples. X-ray confirmation of the identification is needed since it is possible that Mn_5O_8 formed upon ion-bombardment during sample preparation or upon exposure to the electron beam. (2) Aligned intergrowth of monoclinic Mn_5O_8 in secondary pyrolusite may be responsible, along with oriented micropores, for the nontetragonal characteristics displayed by such pyrolusite. (3) Intergrowths of Mn_5O_8 and pyrolusite were found in heated and in unheated samples. The low-temperature occurrence of Mn_5O_8 with pyrolusite and manganite suggests that Mn_5O_8 may be formed together with pyrolusite during the diagenetic decomposition of manganite. Well-crystallized Mn_5O_8 , seen in heated samples, corresponds to a previously documented occurrence of Mn_5O_8 as a compositionally intermediate phase between MnO_2 and Mn_2O_3 above 300°C. (4) A new phase has been found that has a diffraction pattern related to the pyrolusite [010] pattern, but that contains reflections corresponding to spacings three times that of the pyrolusite (101) planes. Ordering of OH groups and Mn atoms with different oxidation states across the (101) planes of the structure may explain these reflections. If so, this phase has a stoichiometry intermediate between $MnOOH$ and MnO_2 .

ACKNOWLEDGMENTS

The authors would like to thank G. E. Brown, Jr., for providing us with samples. We also thank Barbara Miner, Reinhard Neder, Gerard Spinnler, Theresa Keegan, John Wheatley, and Shirley Turner for their assistance in various aspects of this study. Helpful reviews of this paper were provided by R. G. Burns, Rudolf Giovanoli, and R. J. Reeder. Funding was provided by NSF Grants OCE-8200118 and OCE-8401107. Electron microscopy was performed at the HRTEM Regional Facility in the Center for Solid State Science at Arizona State University.

REFERENCES

- Baur, W.H. (1976) Rutile-type compounds. V. Refinements of MnO_2 and MgF_2 . *Acta Crystallographica*, B32, 2200–2204.
- Buerger, M.J. (1936) The symmetry and crystal structure of manganite, $Mn(OH)O$. *Zeitschrift für Kristallographie*, 95, 163–174.
- Burns, R.G., and Burns, V.M. (1979) Manganese oxides. In R.G. Burns, Ed. *Marine minerals*. Mineralogical Society of America Reviews in Mineralogy, 6, 1–46.
- Champness, P.E. (1971) The transformation manganite – pyrolusite. *Mineralogical Magazine*, 38, 245–248.
- Dasgupta, D.R. (1965) Oriented transformation of manganite during heat treatment. *Mineralogical Magazine*, 35, 131–139.
- Davis, R.J. (1967) Some manganese oxide pseudomorphs. *Mineralogical Magazine*, 36, 274–279.
- Dent Glasser, L.S., and Smith, I.B. (1968) Oriented transformations in the system $MnO-O-H_2O$. *Mineralogical Magazine*, 36, 976–987.
- de Wolff, P.M. (1959) Interpretation of some γ - MnO_2 diffraction patterns. *Acta Crystallographica*, 12, 341–345.
- Feitknecht, Walter. (1964) Einfluss der Teilchengröße auf den Mechanismus von Festkörperreaktionen. *Journal of Pure and Applied Chemistry*, 9, 423–440.
- Giovanoli, Rudolf, and Leuenberger, U. (1969) Über die Oxydation von Manganoxidhydroxid. *Helvetica Chimia Acta*, 52, 2333–2347.
- Giovanoli, Rudolf, Mauer, R., and Feitknecht, Walter. (1967) Zur Struktur des γ - MnO_2 . *Helvetica Chimia Acta*, 50, 1072–1080.
- Klingsberg, Cyrus, and Roy, Rustum (1959) Stability and interconvertibility of phases in the system $Mn-O-OH$. *American Mineralogist*, 44, 819–838.
- (1960) Solid-solid and solid-vapor reactions and a new phase in the system $Mn-O$. *American Ceramic Society Journal*, 43, 620–626.
- Kozawa, Akiya. (1981) Data, useful information, articles, etc. on MnO_2 collected by the IC MnO_2 office. In B. Schumm, H.M. Joseph, and A. Kozawa, Eds. *Manganese dioxide symposium*, Tokyo, 1980, 2, 559–599. The Electrochemical Society, Cleveland, Ohio.
- Oswald, H.R., and Wampetich, M.J. (1967) Die Kristallstrukturen von Mn_3O_8 und $Cd_2Mn_3O_8$. *Helvetica Chimia Acta*, 50, 2023–2034.
- Oswald, H.R., Feitknecht, Walter, and Wampetich, M.J. (1965) Crystal data of Mn_3O_8 and $Cd_2Mn_3O_8$. *Nature*, 207, 72.
- Pashley, D.W., Menter, J.W., and Bassett, G.A. (1957) Observation of dislocations in metals by means of Moiré patterns on electron micrographs. *Nature*, 179, 752–755.
- Potter, R.M., and Rossman, G.R. (1979) The tetravalent manganese oxides: Identification, hydration, and structural relationships by infrared spectroscopy. *American Mineralogist*, 64, 1199–1218.
- Strunz, Hugo. (1943) Beitrag zum Pyrolusitproblem. *Naturwissenschaften. Wochenschrift für die Fortschritte, der Naturwissenschaft, der Medizin und der Technik.*, 31, 89–91.
- Turner, Shirley, and Buseck, P.R. (1981) Todorokites: A new family of naturally occurring manganese oxides. *Science*, 212, 1024–1027.

MANUSCRIPT RECEIVED JUNE 1, 1985

MANUSCRIPT ACCEPTED JANUARY 17, 1986